Atmospheric Environment 202 (2019) 269–280

Contents lists available at ScienceDirect

Atmospheric Environment

journal homepage: www.elsevier.com/locate/atmosenv

Ozone source apportionment over the Yangtze River Delta region, China: Investigation of regional transport, sectoral contributions and seasonal differences

Li Li[a,b,**,1], Jingyu An[b,1], Ling Huang[a], Rusha Yan[b], Cheng Huang[b,*], Greg Yarwood[c,d]

[a] School of Environmental and Chemical Engineering, Shanghai University, Shanghai, 200444, China
[b] State Environmental Protection Key Laboratory of the Cause and Prevention of Urban Air Pollution Complex, Shanghai Academy of Environmental Sciences, Shanghai, 200233, China
[c] Ramboll China, Shanghai, 200020, China
[d] Ramboll, Novato, CA, 95995, USA

ARTICLE INFO

Keywords:
Ozone
Source contributions
Yangtze River Delta

ABSTRACT

With the stringent emission control measures implemented in recent years, the overall air quality in China has been improved greatly. However, high ozone (O_3) concentrations have become a more and more severe air pollution issue in the rapidly developing Yangtze River Delta (YRD) region of eastern China including Shanghai, Jiangsu, Zhejiang and Anhui provinces. The 90th percentile of O_3-8 h concentration in the YRD region increased from 144 μg/m^3 in 2013 to 168 μg/m^3 in 2017. To investigate the sources of O_3 within the YRD region, we use a tagged-species method in the Comprehensive Air Quality Model with Extensions (CAMx) called Ozone Source Apportionment Technology (OSAT) to quantify O_3 contributions by source regions and sectors in Spring, Summer and Fall. We find that the O_3 pollution in Shanghai, southern Jiangsu and northern Zhejiang is caused by the joint effect of local to regional precursor emissions combined with super-regional O_3 transport. However, these contributions vary among seasons and pollution events. Super regional transport is the major contributor to average O_3 concentration while local and upwind adjacent area contributions can dominate during high O_3 concentration episodes. Source sector analysis indicates that industry and vehicle emissions are major anthropogenic sources. Within the industrial sector, power plants, boilers, and petroleum industry are the top three contributors. Reducing super-regional O_3 transport is of the most importance to lowering the O_3 background but local to regional precursor emission reductions are also of great significance to control O_3 episodes with collaboration at the regional level offering potential for synergistic benefits to adjacent cities.

1. Introduction

With the stringent emission control measures implemented in recent years, the air quality in China has been improved greatly (Avander et al., 2017; Qin et al., 2017). In particular, ambient $PM_{2.5}$ (particulate matter with dynamic equivalent diameter less than 2.5 μm) concentrations have been decreased year by year (Liang et al., 2015). However, high ozone (O_3) concentrations are becoming a more and more severe problem in eastern China (Wang et al., 2017). O_3 is a secondary pollutant formed via photochemical reactions among precursors including nitrogen oxides (NO_x) and volatile organic compounds (VOC) under solar radiation that contributes to the atmospheric oxidation capacity (Finlayson-Pitts and Pitts, 1993), harms human health (Liu et al., 2013; Shao et al., 2006) and ecological environment (Feng et al., 2014, 2015).

The Yangtze River Delta (YRD) region, including Shanghai, Jiangsu, Zhejiang and Anhui provinces, is one of the fast-developing city-clusters in China. During 2013–2017, the annual $PM_{2.5}$ concentration decreased from 67 μg/m^3 to 44 μg/m^3 but the 90th percentile O_3-8 h concentration increased from 144 μg/m^3 to 168 μg/m^3 based on the data released by the Ministry of Ecology and Environment of the People's Republic of China (http://www.mep.gov.cn). During the Summer of 2013–2017, high O_3 pollution episodes frequently occurred over the YRD region under effect of the subtropical anticyclone. For example, from July

* Corresponding author.
** Corresponding author. School of Environmental and Chemical Engineering, Shanghai University, Shanghai, 200444, China.
E-mail addresses: lili10010844@shu.edu.cn (L. Li), huangc@saes.sh.cn (C. Huang).
[1] These two authors contributed equally to this work.

https://doi.org/10.1016/j.atmosenv.2019.01.028
Received 1 March 2018; Received in revised form 16 January 2019; Accepted 19 January 2019
Available online 23 January 2019
1352-2310/

25^{the} to August 1st, 2015, the O_3-1 h max concentrations exceeded the national ambient standard of 200 μg/m^3 with a peak value reaching 269.5 μg/m^3 and fraction of hours exceeding the 1-h standard reaching 34.7%.

Model projections indicate that O_3 pollution is likely to worsen in the future (Wang et al., 2013; Turnock et al., 2018). In previous studies, various ozone source apportionment methods including the brute force method, the integrated process analysis, response surface modeling, and the ozone source apportionment techniques have been applied to better understand the ozone pollution sources (Gao et al., 2016; Han et al., 2018; Li et al., 2012a, 2012b, 2013; Liu et al., 2010; Ou et al., 2016; Qu et al., 2014; Wang et al., 2009a; Xing et al., 2011; Zhang et al., 2016). However, most of the studies focused on specific ozone episodes; thus, the results are applicable for specific cases. Some of the previous studies on regional transport are on provincial level, and the number of emission sources considered is limited. In recent years, O_3 precursor emissions are changing rapidly due to stringent control measures. Therefore, it is important to fully understand the O_3 sources, including regional transport and sectoral contribution, based on an updated emissions inventory. In this study, we did a comparative study among different seasons and divided the regions into subregions to better understand the influences of regional transport; in addition, we included emission sectors up to 17 types. These results can provide scientific support for the prevention and control of O_3 pollution in the YRD region with more details.

2. Methodology

We use a tagged-species method in the Comprehensive Air Quality Model with Extensions (CAMx, http://www.camx.com) called Ozone Source Apportionment Technology (OSAT; Yarwood et al., 1996; Dunker et al., 2002) to quantify O_3 contributions by emission region and source sector. Up to now, the OSAT methodology has been through three versions: OSAT 1 (release in CAMx 1.1 in 1996); OSAT 2 (release in CAMx 4.2 in 2005) and OSAT 3 (release in CAMx 6.3 in 2015). OSAT uses tracers, alternatively referred to as tagged species, to account for contributions to O_3 formation. O_3 formation involves both NOx and VOC and OSAT tracers (N_i and V_i) apportion model concentrations of NOx and VOC to an emission source, i. When O_3 is produced, the increment in O_3 concentration is apportioned by OSAT tracers (O_3N_i and O_3V_i) depending upon the precursors present (N_i and V_i) and whether the O_3 formation was controlled more by the availability of VOC or NOx. The OSAT O_3 tracers (O_3N_i and O_3V_i) also track the O_3 that enters CAMx through boundary conditions (BC) or initial conditions (IC). Photochemistry can also destroy O_3, e.g., titration by fresh NO emission or reaction with HO_2 radical, in which case OSAT reduces all O_3 tracers proportionately to account for the increment of O_3 destruction. Consequently, O_3 apportionments from OSAT are always positive (during O_3 formation) or zero (during O_3 destruction) which differs from source sensitivity methods (e.g., brute-force emission perturbations or the decoupled direct method; Dunker et al., 2002) in which O_3 sensitivity to emissions can be negative, as discussed by Clappier et al. (2017). The sum of OSAT O_3 tracers is always equal to the CAMx O_3 concentration and thus O_3N_i and O_3V_i always provide a complete apportionment of O_3 to the emission sources, BC and IC. OSAT3 includes an improved approach to handle NOx recycling (Yarwood and Koo, 2015) and improves the accuracy of the OSAT methods by keeping track of the sources of ozone removed by reaction with NO to form NO_2 and subsequently returned as ozone when NO_2 is destroyed by photolysis. Tracking source attribution of nitrogen through all forms of NOy enables OSAT3 to account for NOx recycling when NOx is converted to another form of NOy (e.g., PAN or HNO_3) and later converted back to NOx. OSAT3 uses 10 tracers by source region/group. Detailed information about the OSAT scheme for ozone apportionment can be referred to the literature (Yarwood et al., 1996; Yarwood and Koo, 2015; http://www.camx.com/files/camxusersguide_v6-40.pdf).

Table 1
WRF physics options.

Physics Option	D01(36 km)& D02(12 km)
Microphysics	Lin et al. scheme
Longwave radiation	RRTM scheme
Shortwave radiation	Goddard shortwave
Surface layer	MM5 similarity
Land surface	Noah Land Surface Model
Planetary Boundary Layer	Yonsei University scheme
Cumulus Parameterization	Grell 3D

The Sparse Matrix Operator Kernel Emissions (SMOKE) model is applied to process regional emission input from different sources and the Weather Research and Forecasting (WRF) model provides meteorological inputs. The geographic source areas for OSAT and receptors for analysis are zoned and labelled using ArcGIS based on vectorized regional geographical information.

2.1. WRF model setup

The WRF (version 3.9.1.1) meteorological modeling domain consists of two nested Lambert projection grids with resolution of 36 km (D01) and 12 km (D02), respectively. WRF was run for the two domains with two-way feedback. The D01 domain was used to resolve the larger scale synoptic weather systems while the D02 grid resolved the finer details of atmospheric conditions and was used to drive the O_3 simulations. Both domains utilized 27 vertical sigma layers (Table S1), with major physics options for each domain listed in Table 1.

Initial and boundary conditions (IC/BCs) for WRF modeling were based on the 1-degree by 1-degree FNL Operational Global Analysis data that are archived at the Global Data Assimilation System (GDAS). Boundary conditions were updated at 6-h intervals for D01.

2.2. CAMx model setup

CAMx model coupled with OSAT3 is applied in this study with two-way nested domains. The parent domain covers the entire China with a horizontal grid resolution of 36-km and the nested domain covers the YRD region with a grid resolution of 12-km. Both domains are based on the same projection for WRF modeling. The 27 vertical layers from WRF were mapped to 14 vertical layers for CAMx extending from the surface to 100 mb.

The O_3 modeling was done using CAMx version 6.4, released by Ramboll (http://www.camx.com) in December 2016. The Carbon Bond 2005 chemistry mechanism (CB05), RADM aqueous chemistry, ISORROPIA inorganic aerosol chemistry scheme and the SOAP secondary organic aerosol scheme were selected as the chemical mechanism for CAMx simulations. Chemical boundary conditions for the outer 36-km domain were extracted from the global chemical transport model for O_3 and related chemical tracers, version 4 (MOZART-4; Emmons et al., 2010). The inner 12-km domain simulation was coupled to the 36-km domain simulation by 2-way nesting.

CAMx simulations were conducted for May (refers to Spring), August (refers to Summer), and October (refers to Fall) in 2015, respectively, to trace the O_3 formation and source contribution. Each simulation included a three-day spin-up period. Within the 12-km domain, we set up eight source regions for OSAT analysis (Fig. 1) including northern Jiangsu (NJ), southern Jiangsu (SJ), Shanghai (SH), northern Zhejiang (NZ), southern Zhejiang (SZ), Anhui (AH), regions inside 12-km domain (Peripheral Region) and regions outside 12-km domain referring to super regional transport (SRT). In addition, to figure out the contributions from local city to the receptors, we separated the city where the receptor locates from the above sub-region and named “local”. Based on the emissions inventory, five source categories are identified for OSAT analysis including combustion, industry,

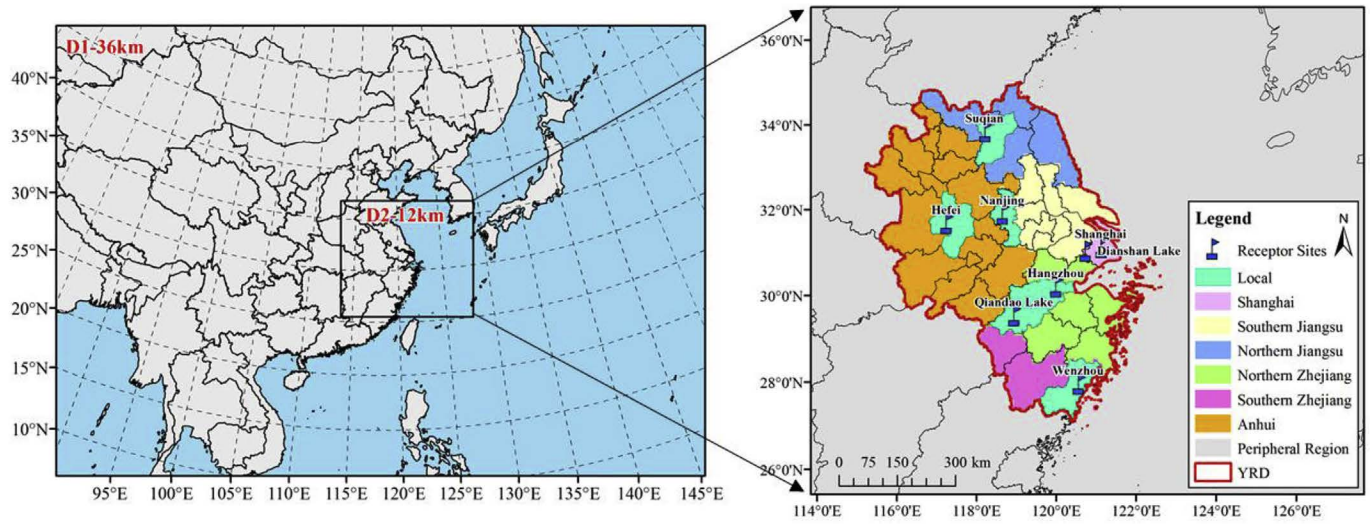

Fig. 1. CAMx 36-km and 12-km modeling domains with OSAT source regions.

mobile, residential and biogenic emissions. Eight receptors including Shanghai, Suqian, Nanjing, Hangzhou, Hefei, Wenzhou, Qiandao Lake, and Dianshan Lake are selected to analyze O_3 formation and source contribution from different regions. The selection of these receptors can be classified into three types: Type1: provincial capitals, which represent typical urban area, Shanghai (provincial city), Nanjing (capital of Jiangsu province), Hangzhou (capital of Zhejiang province), Hefei (Capital of Anhui province); Type2: since the provincial capitals are mainly concentrated in the central YRD region, we add another two urban sites located in the northern and southern region, including Suqian (northern) and Wenzhou (southern); Type3: since O_3 formation is different between urban and rural area, we also select two typical rural sites including Dianshan Lake and Qiandao Lake, with little anthropogenic precursor emissions in the nearby surrounding region. Locations of these receptors range from north to south, from urban to rural (Fig. 1).

The emissions inventory for the 36-km domain was based on the MEIC-2012 developed by Tsinghua University (http://www.meicmodel.org/). Detailed information about the emissions inventory over the parent domain can be found in previous literature (Li et al., 2017). The emissions inventory for the YRD region was based on a most recent inventory developed by our group (Huang et al., 2011; Li et al., 2017; Liu et al., 2018). The updated emissions inventory is divided into five source categories including combustion, industry, mobile, residential and biogenic emissions. Lumping of detailed sectors into those five categories is shown in Table 2.

Table 2
Lump of the emission sectors.

Category	Source sectors
Combustion	Powerplant
	Boiler
Industrial source	Cement
	Iron and Steel
	Petrol chemical industry
	Other industrial processing sources
	Automobile manufacturing
	Rubber and Plastic
	Textile
	Other industrial solvent use
Mobile source	Diesel vehicle
	Gasoline vehicle
	Non-road
Residential source	Domestic solvent use
	Dry cleaning
	Other residential source
Biogenic source	Biogenic emissions

3. Model verification

3.1. Evaluation of WRF predicted meteorological parameters

WRF predicted surface temperature, wind speed, wind direction, and relative humidity from the 12-km domain were validated against hourly observations at 6 surface stations over the YRD region. Observational data for the surface stations were obtained from the airport meteorological database (http://www.weatherunderground.com/). Several quantitative performance metrics were used to compare hourly surface observations and model estimates: mean bias (MB), mean error (ME), root mean square error (RMSE), mean fractional bias (MFB), index of agreement (IOA) and correlation coefficient (R) based on recommendations of Emery et al. (2017) and Simon et al. (2012). A summary of these statistics by station is shown in Table S1. Distribution of hourly mean bias and mean error are shown in Fig. S1.

Temperature shows good agreement between observations and simulations at all sites with IOA values above 0.85 and bias ranging from −1.75–1.33 K. Mean bias of relative humidity ranges from −12.07 to 7.17, with the largest bias occurring at Hefei in October. Wind speed biases are generally positive except for Shanghai Hongqiao in August and October, with the smallest bias occurring at Shanghai Pudong in October (−0.01 m/s) and the largest bias at Hangzhou in August and October (1.35 m/s). These results are comparable with other recent WRF modeling efforts in YRD investigating O_3 formation (Dong et al., 2013; Zhang et al., 2015; Li et al., 2012a,b) and therefore is reasonable.

3.2. Ozone simulation and evaluation

Observed hourly O_3 concentrations from the China Air Quality Release System (http://106.37.208.233:20035/) were used to evaluate O_3 modeling performance for different cities within the YRD region. A number of statistical metrics was used to evaluate the model performance, including normalized mean bias (NMB), normalized mean error (NME), mean fractional bias (MFB), mean fractional error (MFE), and Index of agreement (IOA). Equations of these metrics are shown in the SI.

Table S2 shows the statistical parameters for daily average 8-h (9:00–16:00) O_3 concentrations. Model performance statistics shown in Table S2 are consistent with previous studies in the YRD region (Gao

et al., 2016; Wang et al., 2009b; Li et al., 2011, 2012a,b, 2016) and elsewhere in China (Li et al., 2013; Shen et al., 2015; Wang et al., 2015; Wu et al., 2012; Tang et al., 2011). Among these statistical parameters, Index of Agreement (IOA) for simulation results in each month across cities are all above 0.7, indicating that this model system exhibits high level of consistency for O_3 simulations. Emery et al. (2017) recommended NMB lower than 15%. All cities except Shanghai meet this criterion for 3-month average O_3 concentration. There is consistent low bias for Shanghai, which could be due to two reasons: (1) emissions inventory for NOx might be overestimated, as indicated by the NO_2 model performance in Table S3, while VOCs emissions may be underestimated; (2) Shanghai is more likely to be influenced by the coastal meteorology, for which a 4-km grid will be needed to resolve the impact from coastal meteorology.

Figure S2 denotes the time series of comparison between predicted O_3 concentrations and hourly observations. Predicted O_3 concentrations are generally consistent with observations in terms of magnitudes and temporal variations, which indicates that simulations can well demonstrate the changing courses of O_3 over the YRD region.

4. Results and discussions

4.1. Meteorological conditions for different seasons

The simulated spatial distributions of average wind speed and direction, temperature, and daily maximum 8-h (MDA8) O_3 concentrations in different seasons over the YRD Region are presented in Fig. 2. Differences exist in the spatial distribution of O_3 concentrations over YRD and meteorological condition is an important influencing factor, especially the wind. The temperature difference (~4 °C) is small within the YRD region in each season. However, high O_3 concentration areas appear in the northwest region in Spring and Summer, and in southwest in Fall. According to the spatial distributions of wind direction in YRD, the prevailing wind is south-eastly in Spring and Summer, while it is north-eastly in Fall, and those regions with high O_3 concentrations are located in the downwind area.

4.2. Regional contribution to O_3 by season

4.2.1. Spring

Fig. 3 shows the contributions from regional sources to hourly O_3 concentrations at each receptor in Spring. Regarding the regional sources of total O_3 concentrations in Spring in Shanghai, super-regional transport has a relatively large contribution to MDA8 with proportions exceeding 70%. During periods of high O_3 level in Shanghai (e.g. May 19th), local sources have a significantly larger contribution (e.g. exceeding 20% during 13:00–14:00). Meanwhile, surrounding areas of Shanghai including southern Jiangsu and norther Zhejiang also have a consistent increasing contribution, which indicates that high events are mainly driven by core areas including Shanghai, southern Jiangsu and northern Zhejiang within the YRD region.

Among receptors within Jiangsu Province, cities including Suqian and Nanjing are discussed. Suqian, located in northern Jiangsu, has a generally higher level of O_3 than Shanghai in Spring. Regional O_3 contributions in Suqian are associated with the directions of the prevailing wind in the YRD Region. Around May 19th, Anhui contributes significantly to O_3 concentrations in Suqian during the pollution episode (by 15.2%), while from May 23rd to May 27th, local sources have a significant contribution during this continuous pollution episode, with a contribution from northern Jiangsu (by 8.4%) and southern Jiangsu (by 4.9%). On average, surrounding areas of Suqian including northern Jiangsu and southern Jiangsu exhibit noticeable contribution to O_3 concentrations in Suqian. Nanjing is located in southern Jiangsu. Regional sources from southern Jiangsu have an average contribution of around 10% to O_3 concentrations in Nanjing, exceeding local sources. Northern Zhejiang and Anhui also have a relatively high contribution during certain periods as influenced by prevailing winds. Similar to Shanghai and Suqian, sources from local and surrounding areas have a larger contribution to O_3 concentrations in Nanjing during a high O_3 period (May 23rd to May 26th).

In Hefei of Anhui province, local sources contribute to MDA8 by around 8.0%, while the rest areas of Anhui province have similar contribution of around 8% to O_3 concentrations. Under the influence of prevailing winds in Spring, O_3 concentrations in Hefei are also affected by sources in southern Jiangsu and northern Zhejiang.

Among receptors within Zhejiang Province, from north to the south, two urban cities including Hangzhou and Wenzhou are discussed. In Hangzhou, local sources contribute to MDA8 by 6.5%. External influential areas are mainly northern Zhejiang with an average contribution of around 10%, followed by southern Jiangsu. In Wenzhou, local sources contribute to MDA8 and maximum hourly concentrations by around 6.3% and 8.7%, respectively. Northern Zhejiang contributes significantly to Wenzhou during certain pollution episodes, with an average contribution of around 4.0% to MDA8.

Qiandao Lake (QDL) and Dianshan Lake (DSL) are two rural receptors located in northern and southern YRD, respectively. At QDL, super-regional sources contribute to O_3 concentrations by around 70%. Inside the YRD region, sources in the local area and northern Zhejiang have the largest contribution to O_3, with an average contribution to MDA8 taking up 8.4% and 3.9%, respectively. Southern Jiangsu and southern Zhejiang also show noticeable contribution to O_3 concentrations at QDL during certain periods. DSL is located at the junction of Jiangsu, Zhejiang and Shanghai, of which O_3 concentrations are influenced by southern Jiangsu, northern Zhejiang and Shanghai. During the pollution episode around May 19th, all those areas possess significant contribution. Shanghai, northern Zhejiang and southern Jiangsu have an average contribution to MDA8 of 8.1%, 7.7%, 5.9%, respectively.

In general, super-regional transport has the largest contribution, while local area where the receptor is located and its surrounding upwind areas have significantly larger contribution to O_3 concentrations during high O_3 period in Spring season. This indicates that local O_3 formation is a key factor to the high-level O_3. Comparisons between urban stations and rural stations indicate that O_3 sources at rural stations are more influenced by their surrounding areas.

4.2.2. Summer

Fig. 4 shows contribution distributions of regional sources to hourly O_3 concentrations at each receptor in Summer. In Shanghai, super-regional background has a relatively smaller contribution to MDA8, with proportions around 50%, compared with Spring. In combination with the distributions of regional contribution time series, during the pollution episode from August 1st to 6th, local areas, northern Zhejiang and southern Jiangsu are the main contributors, while during the pollution episode around August 28th, southern Jiangsu and Anhui contribute more to O_3 in Shanghai. Regarding the distributions of MDA8 contributions, Shanghai, northern Zhejiang and southern Jiangsu contribute by 11.4%, 12.4% and 6.2%, respectively.

Among receptors within Jiangsu Province, cities including Suqian and Nanjing are discussed for Summer. In Suqian, the main contributing areas differ by pollution episodes, which is similar to Shanghai. The pollution episode in early August is mainly influenced by transport from Anhui, while the pollution episode around August 13th is significantly influenced by southern Jiangsu. Northern Jiangsu has a relatively consistent contribution during other periods of time. Regarding the distributions of average contributions, local sources and northern Jiangsu have a contribution of around 10% and 9%, respectively. The distributions of regional sources in Nanjing during several O_3 pollution episodes are similar to those in Suqian. The pollution episode in early August is mainly influenced by transport from Anhui, while the pollution episode around August 13th is significantly influenced by southern Jiangsu. Southern Jiangsu has a relatively consistent contribution during other periods of time. Regarding the distributions

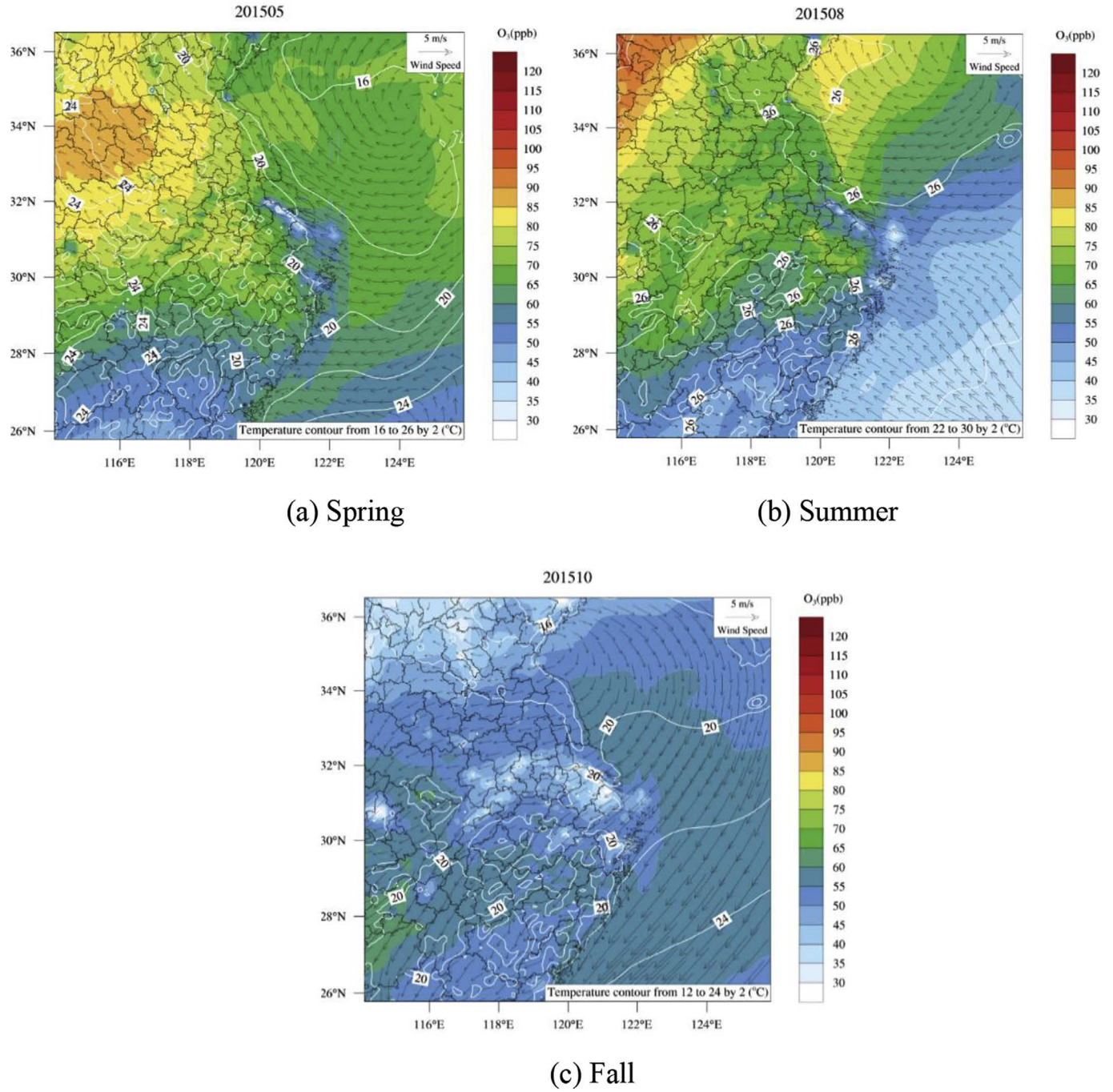

Fig. 2. Model predicted average wind speed and direction, temperature and daily maximum 8-h O_3 concentrations for (a) Spring, (b) Summer, and (c) Fall over the YRD region.

of average contributions, local sources, southern Jiangsu and Anhui are the main O_3 regional source contributors inside the region with a proportion of around 8%, 13% and 11%, respectively.

Close to Nanjing in terms of the location, Hefei also shows a similar O_3 transport pattern to Nanjing. Local sources in Hefei, southern Jiangsu and Anhui are the main contributors to O_3 sources, with average contribution to MDA8 of 10.5%, 9.3% and 10.0%, respectively.

Among urban receptors in Zhejiang province, local contributions have a larger proportion in Hangzhou than in Nanjing. The pollution episode in early August is mainly influenced by local sources, while the pollution episode at the end of August is significantly influenced by Hangzhou's adjacent areas in northern Zhejiang. Regarding the distributions of average contributions, local sources in Hangzhou have an average contribution to MDA8 of around 15.5%, followed by regional contributions of northern Zhejiang taking up around 12.4%. In Wenzhou, the pollution episode in early August is mainly caused by local contributions as well as other regional transport from the surrounding southern Zhejiang region. During the pollution episode around August 25th, southern Jiangsu and northern Zhejiang have noticeable contributions to O_3 in Wenzhou. Local sources in Wenzhou contribute by around 23.6%.

Among the two rural receptors, at QDL, the pollution episode in early August is influenced by local sources, southern Jiangsu and other areas inside its surrounding southern Zhejiang region, while during the pollution episode at the end of August, Anhui and northern Zhejiang have more contributions. Regarding the average contributions to

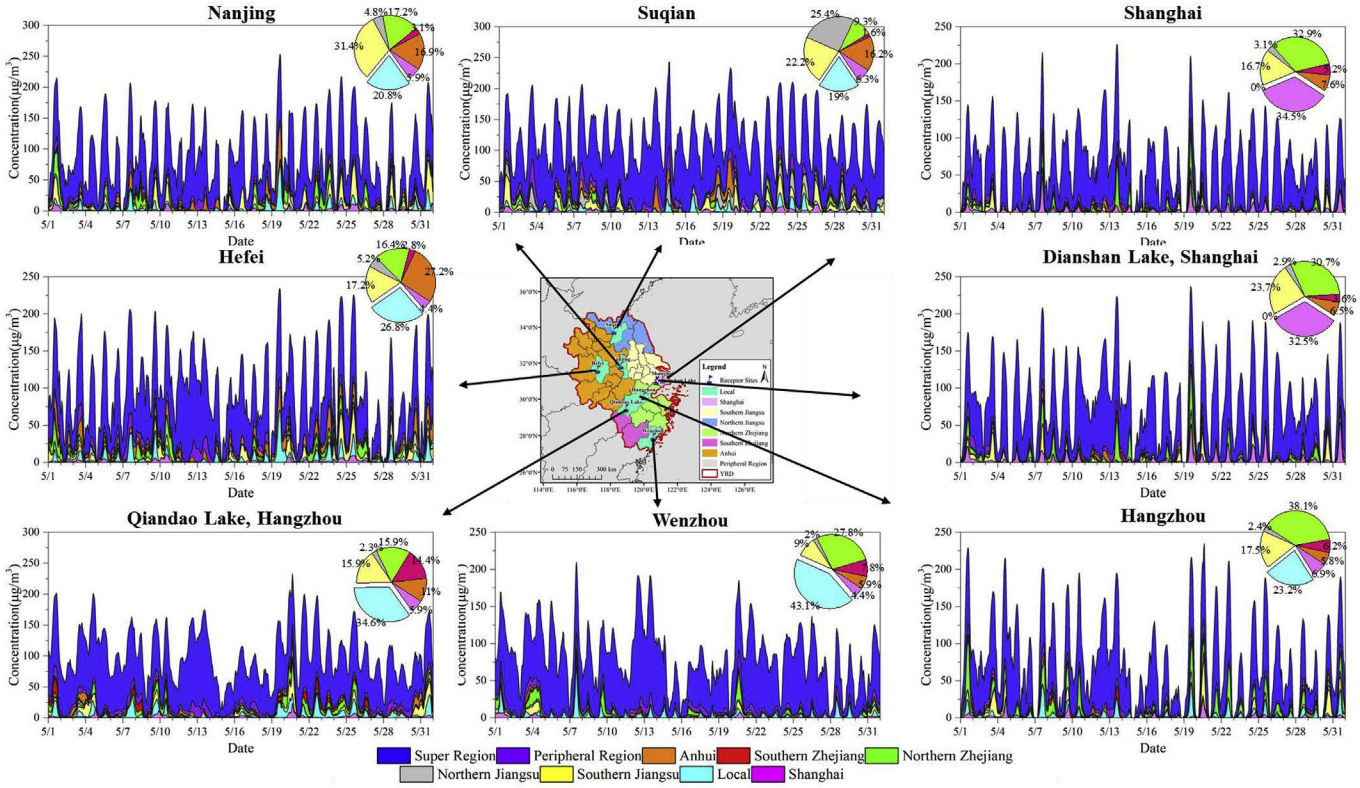

Fig. 3. Contribution of regional sources to hourly ozone concentrations at each receptor over the YRD Region in May 2015.

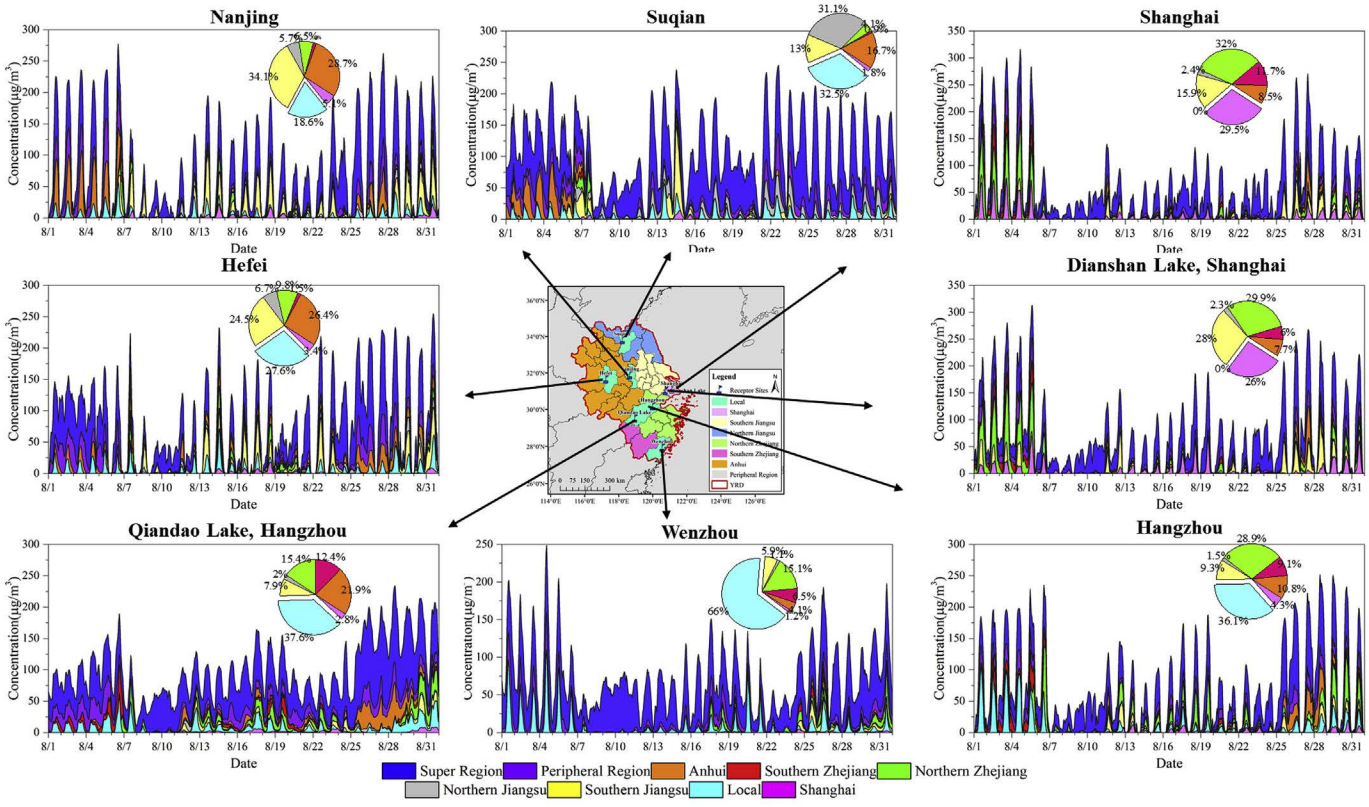

Fig. 4. Contribution of regional sources to hourly O_3 concentrations at each receptor over the YRD Region in August 2015.

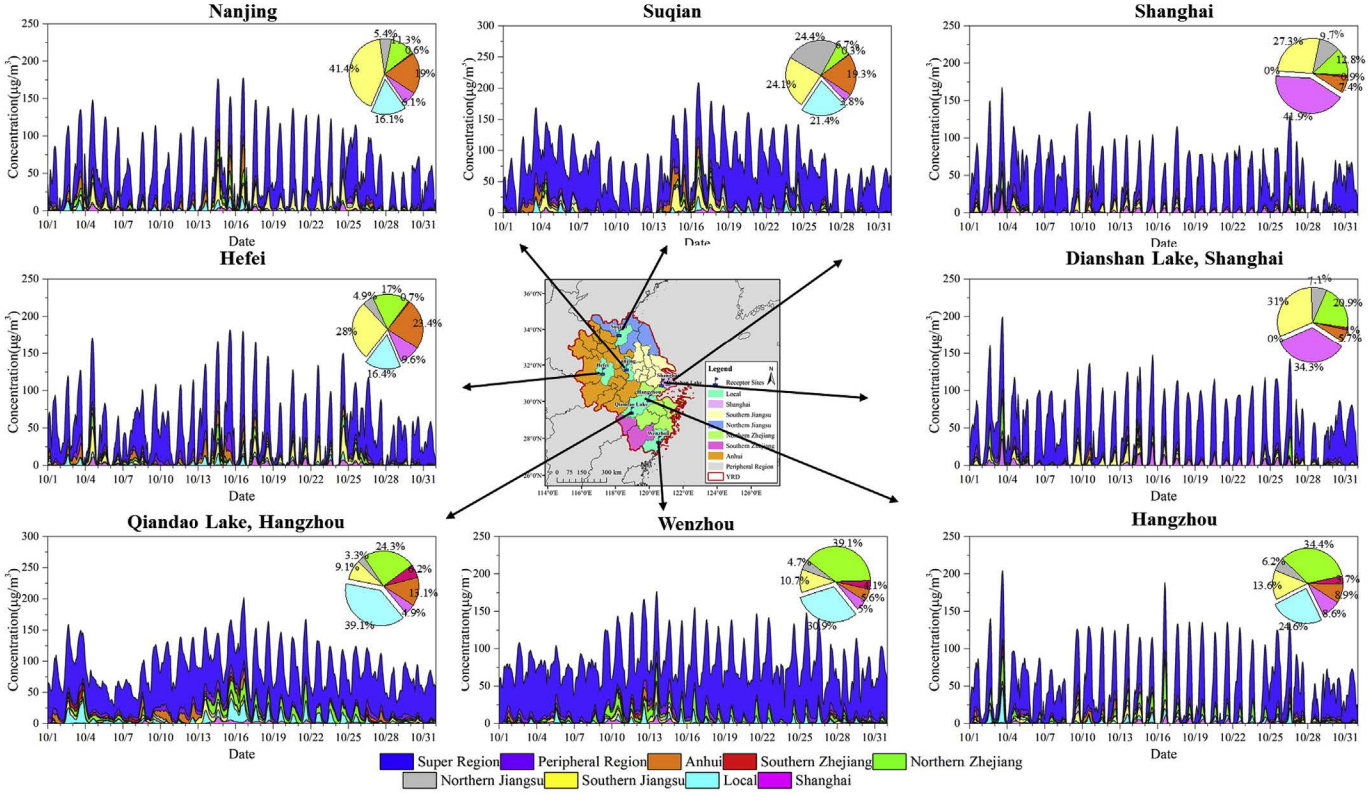

Fig. 5. Contribution of regional sources to hourly O_3 concentrations at each receptor over the YRD Region in October 2015.

MDA8, local sources, Anhui and northern Zhejiang contribute by around 13.1%, 7.7% and 5.4%, respectively. At DSL, the pollution episode in early August is mainly influenced by northern Zhejiang, while during the pollution event at the end of August, southern Jiangsu has a more significant contribution. In terms of the average contributions to daily maximum hourly concentrations, northern Zhejiang, southern Jiangsu and local sources in Shanghai have contributions of 12.2%, 11.5% and 10.1%, respectively.

In general, super-regional transport have the largest O_3 contribution to the YRD region in Summer. Compared with results in Spring, contribution from super-regional transport is much lower in Summer. During different pollution episodes in Summer, O_3 contributing areas differ under the influence of prevailing wind directions. During the pollution episode in early August, the prevailing winds are from the south, suggesting that O_3 concentration is more influenced by southern upwind areas. On the contrary, during the pollution episode at the end of August, the prevailing winds are from the west, indicating that western upwind areas contribute more to O_3. Regarding the comparison between urban and rural receptors, O_3 sources at rural stations are more cooperatively controlled by their surrounding areas.

Compared with previous study (Li et al., 2016), the contribution of super regional transport in Summer in this study (48.8% to Shanghai 8-h O_3) is higher than the case in 2013 (24.9%). Local contribution from Shanghai in the current study (11.4%) is similar to the previous study (17.6%). Contributions from Jiangsu to urban Shanghai in both studies are small (6.2% and 7.1%, respectively). The contribution from Zhejiang in the current research is lower (4.6% + 12.4% = 17%) than the previous study (36.0%). The reasons are mainly due to four points: (1) regional contribution to O_3 is highly influenced by meteorological conditions, namely case by case. In the previous study, the prevailing wind under different O_3 cases are mainly southerly, causing high influence from Zhejiang. In the current study, the prevailing wind is southern-easterly, causing high influence from outside the domain and lower affect from Zhejiang; (2) an updated version of CAMx is applied and the formulation used in OSAT is updated in this study (CAMx Version 6.4, OSAT3), while the previous study implemented OSAT2 in CAMx version 6.1; (3) emission inventories for the modeling domains have been updated, considering development, changes of emissions sources, and control of the anthropogenic emissions; (4) global boundary conditions extracted from the global model (MOZART) results are take into consideration in this study, which may also increase the super-regional contribution.

4.2.3. Fall

Fig. 5 shows regional contributions to hourly O_3 at each receptor in Fall. In Shanghai, regarding the regional sources of total O_3, super-regional background has an average contribution to MDA8 and daily maximum hourly concentrations around 70%, similar to Spring. In combination with the distributions of regional contribution time series, during the pollution episode in mid-October, southern Jiangsu and northern Zhejiang have more significant contribution, while for the rest period of time, local sources in Shanghai are the main contributor.

Among urban receptors in Jiangsu province, in Suqian, as for the O_3 regional source time series in Fall, Jiangsu contributes most to the high level of O_3 around October 16th. Regarding distributions of average contributions, super-regional transport have the largest impact. In Nanjing, during the mid-October pollution episode, southern Jiangsu, northern Zhejiang and Anhui mainly cause the high level of O_3. In terms of the average contributions, southern Jiangsu is the main contributor to O_3 in Fall, with an average contribution to daily maximum hourly O_3 concentration around 11.1%.

Hefei, as the capital of Anhui province, also shows a similar O_3 transport pattern to Nanjing. Super-regional contributions account for around 70%. Southern Jiangsu has a significant contribution during the period of a high level of O_3. Meanwhile, the rest areas of Anhui also have noticeable contributions.

In Hangzhou, super-regional O_3 background has a contribution around 70%. Northern Zhejiang is the most influential area to O_3

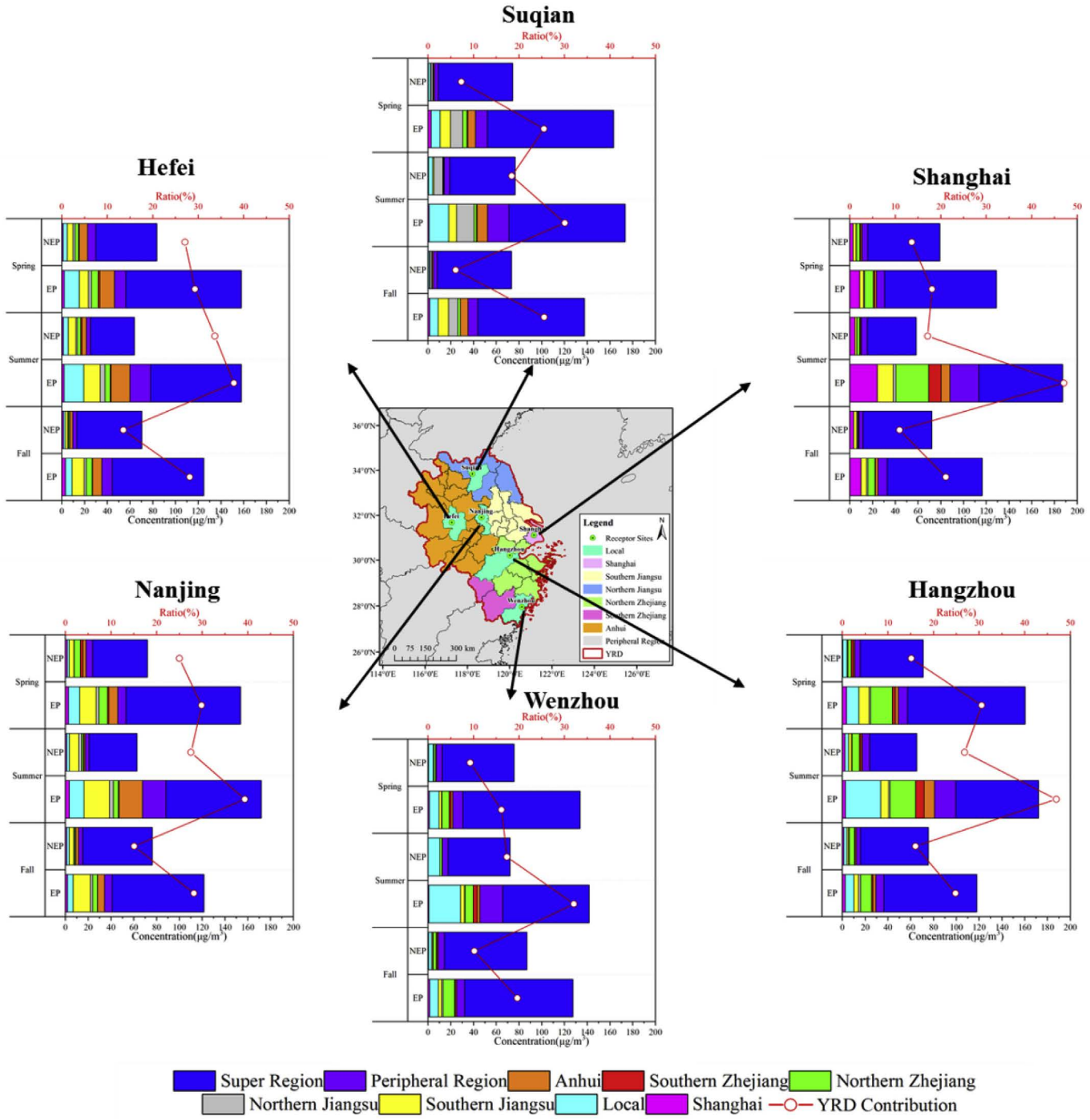

Fig. 6. Comparisons of the regional O_3 transport and YRD contribution to MDA8 over the Yangtze River Delta in three seasons during different period.

concentrations in Hangzhou with an average contribution of 7.4%–9.1%. Under the influence of prevailing wind directions, besides local sources, northern Zhejiang is the largest contributor to MDA8 and daily maximum hourly concentrations in Fall in Wenzhou, taking up around 6.4% and 7.8%, respectively.

At QDL, the pollution episode around October 16th is mainly influenced by local sources and by northern Zhejiang. Regarding average contributions to MDA8, local sources and northern Zhejiang contribute by around 10.5% and 6.9%, respectively. At DSL, regarding the regional contributions over the YRD region, O_3 concentrations are mainly influenced by local sources and southern Jiangsu in Fall. During the pollution event around October 13th, southern Jiangsu has a significant contribution, while during other periods of a relatively low level of O_3, local sources in Shanghai are the main contributors.

In general, super-regional transport have a similar contribution to Spring in Fall. Under the influence of prevailing winds in Fall, northern upwind areas contribute most during periods of high O_3 level. This result shows that the reduction of background O_3 is very important in lowing the O_3 level in YRD region in Spring and Fall seasons.

4.2.4. *Comparisons of regional transport to urban O_3 in different seasons*

Fig. 6 shows the contribution distributions of regional sources and YRD contribution ratio to daily average maximum 8-h concentrations at each receptor in three seasons during different periods, EP (pollution episode) and NEP (not episode) with MDA8 higher and lower than 100 μg/m^3 respectively. Super regional transport is an important source

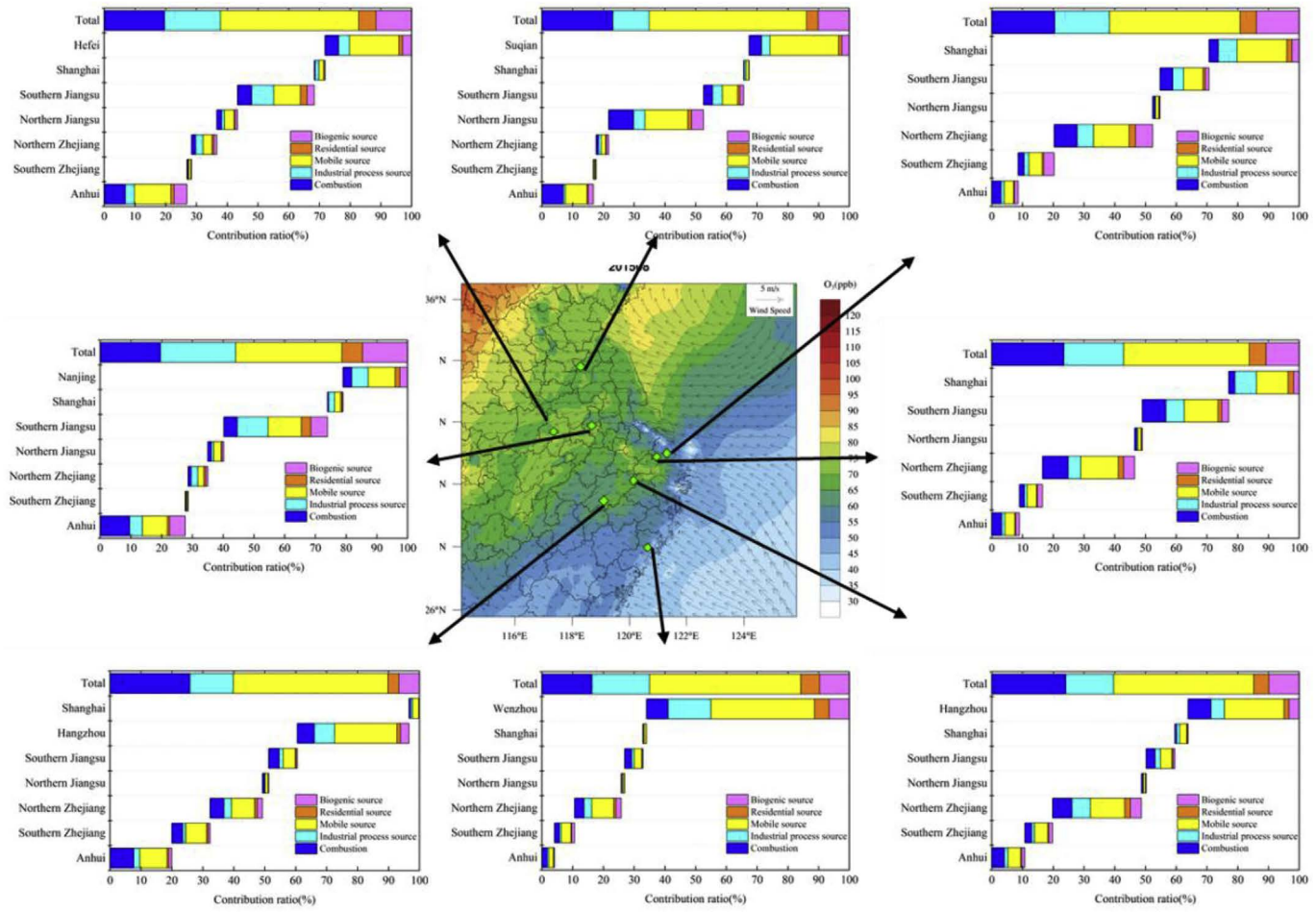

Fig. 7. Regional and sectoral contributions to daily maximum 8-h O_3 concentrations across typical cities over the YRD in August 2015.

of O_3 for all three seasons, and its contribution to MDA8 varies from 38.7 to 111.1 μg/m^3 among seasons and the associated YRD contribution ratio also exists seasonal differences. YRD contribution ranges between 16.1% and 47.1% during EP period, which is higher than NEP period (6.1%–33.7%) and with highest contribution in Summer at each receptor. With respect to sub-region contribution, the sub-region that each city is located in plays more important role. For example, Nanjing is in southern Jiangsu and along east border of Anhui; both these two sub-regions contribute more than 20 μg/m^3 to Nanjing MDA8 in Summer EP periods. When it comes to local city contribution, it also varies among seasons and shows more contribution during EP periods, especially for Summer. The larger proportion of local and regional contribution during high O_3 events indicates that there is full potential for local governments to reduce the high O_3 episode through regional collaboration of controlling emission sources within the YRD region. These results indicate that an O_3 pollution control region is needed in terms of policy implications. In other words, emission control measures should be instructed to the local city as well as the upwind sub-region in order to reduce O_3 pollution episode for that city.

4.3. Sectoral contributions to O_3

Fig. 7 and Fig. 8 shows the regional and sectoral contributions to daily maximum 8-h O_3 concentrations in Summer, and 1-h result is shown in SI Fig. S3. Results show that mobile source is the largest contributor to the urban station in Shanghai with a contribution of 42.5%, among which diesel vehicles and gasoline vehicles contribute the most, followed by stationary combustion sources of 20.5%. Contribution from the combustion sources takes up 20.5% with power plants showing a larger contribution than industrial boilers. Manufacturing process sources have a contribution around 17.8%, among which petrochemicals and chemical industries, and rubber and plastic industries contribute most, resulting total contribution of 10.5%. Biogenic emissions have a contribution of around 14.0%. Results at the Dianshan Lake station are generally similar to those in urban Shanghai with emissions from southern Jiangsu have a more significant contribution among regional sources.

In Suqian, MDA8 O_3 concentrations are mainly influenced by mobile sources and stationary combustion sources with an average contribution taking up around 51.1% and 23.0%, respectively. Among vehicle emissions, diesel vehicles and non-road contribute most, while petrochemicals and chemical industries as well as other solvent use industries contribute most among manufacturing process sources. The total contribution of industrial process source takes up around 11.9%.

In Nanjing, O_3 concentrations are mainly influenced by mobile sources, manufacturing process sources and stationary combustion sources with an average contribution of 35.5%, 23.5% and 20.5%, respectively. Among mobile sources, diesel vehicles and gasoline vehicles contribute most, while petrochemicals and chemical industries take up around 50% among the contributions of manufacturing process sources.

At the urban station in Hangzhou, O_3 concentrations are mainly influenced by mobile source, stationary combustion sources and manufacturing process sources with an average contribution taking up around 45.6%, 24.0% and 15.6%, respectively, which is similar to Shanghai. Among manufacturing process sources, cement industries as well as petrochemicals and chemical industries are the main contributors. Regarding the emission sources at QDL, mobile sources, stationary combustion sources and manufacturing process sources have an

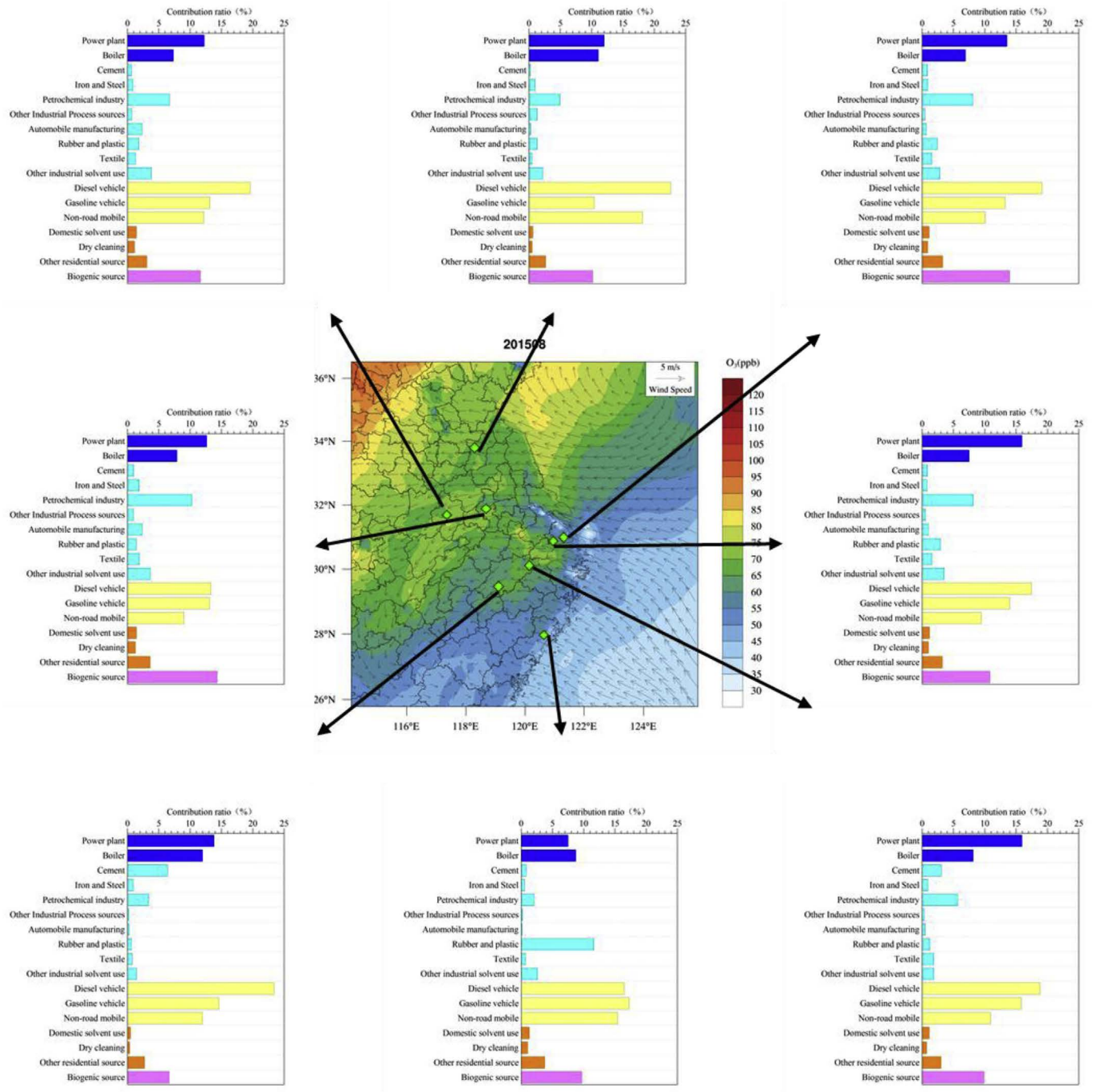

Fig. 8. Detailed sectoral contributions to daily maximum 8-h O_3 across typical cities over the YRD region in August 2015.

average contribution taking up around 50.0%, 25.8% and 14.0%, respectively. Among manufacturing process sources, cement industries as well as petrochemicals and chemical industries are the main contributors. Diesel vehicles have a larger contribution among mobile sources than in urban Hangzhou.

In Wenzhou, MDA8 O_3 concentrations are mainly influenced by mobile sources, stationary combustion sources and manufacturing process sources with an average contribution taking up around 49.2%, 16.3% and 18.7%, respectively. Rubber and plastic industries take up over 60% among the contributions of manufacturing process sources, while diesel vehicles, gasoline vehicles and non-road have equivalent proportions among the contributions of mobile sources.

In Hefei, MDA8 O_3 concentrations are mainly influenced by mobile sources, stationary combustion sources and manufacturing process sources with an average contribution taking up around 44.9%, 19.6% and 18.3%, respectively. Among manufacturing process sources, petrochemicals and chemicals industries, vehicle manufacturing industries and other solvent use sources are three main emitters.

5. Conclusions

O_3 pollution episodes not only occur in Summer but also in Spring and Fall in the YRD region. This research shows that O_3 pollution over the YRD has contributions from local to regional precursor emissions in addition to O_3 super-regional transport. However, the contributions of these O_3 sources vary among seasons and episodes. Our results indicate that the super-regional (or "background O_3") contribution to MDA8 O_3 at urban receptors on clean days ranges from 48 to 65 μg/m^3 in Spring,

39–58 μg/m^3 in Summer, and 57–73 μg/m^3 in Fall. The photochemical O_3 production from precursor emissions from local and regional sources plays a dominant role in the pollution days in Summer, which can increase the O_3 level about 33–78 μg/m^3. Taking only the photochemical O_3 production within YRD into consideration, the contributions from local emission sources range from 19%–43% in Spring, 19%–66% in Summer, and 16%–42% in Fall, indicating that local emissions control is still of priority to reduce O_3 levels, especially during pollution episodes. In addition, contributions from adjacent sub-region usually play an important role during O_3 pollution episodes. Examples of substantial O_3 transport between adjacent sub-regions include southern Jiangsu and Anhui's contribution to Nanjing, northern Jiangsu to Suqian, Anhui to Hefei, northern Zhejiang to Wenzhou, northern Zhejiang to Shanghai, and northern Zhejiang to Hangzhou. These results indicate that coordinating emission control activities in adjacent sub-regions can produce synergistic benefits for reduction of O_3 episodes.

Sectoral source apportionment of O_3 results indicates that industry and vehicle emissions are major anthropogenic precursor sources of O_3. Within the industry sector, power plants, boilers (mainly NOx sources) and petroleum industry (mainly VOCs sources) are top three contributors. Diesel vehicle, gasoline vehicle, and non-road mobile emissions also play important roles in O_3 formation.

These results indicate that coordinated emission control at national level is needed to reduce the O_3 background entering the YRD region. In addition, collaboration among adjacent urban areas is needed to reducing O_3 episodes within the YRD region.

Conflict of interest

The authors declare that there is no conflict of interest regarding the publication of this article.

Acknowledgements

This study was financially supported by the National Natural Science Foundation of China (NO. 41875161), the Key research project from Shanghai Environmental Protection Bureau via grant No. Huhuanke (2016–12) and (2017–02).

Appendix A. Supplementary data

Supplementary data to this article can be found online at https://doi.org/10.1016/j.atmosenv.2019.01.028.

References

Avander, R.J., Mijling, B., Ding, J.Y., Koukouli, M.E., Liu, F., Li, Q., Mao, H.Q., Theys, N., 2017. Cleaning up the air: effectiveness of air quality policy for SO_2 and NO_x emissions in China. Atmos. Chem. Phys. 17, 1775–1789.

Clappier, A., Belis, C.A., Pernigotti, D., Thunis, P., 2017. Source apportionment and sensitivity analysis: two methodologies with two different purposes. Geosci. Model Dev. (GMD) 10, 4245–4256.

Dong, X., Gao, Y., Fu, J.S., Li, J., Huang, K., Zhuang, G., Zhou, Y., 2013. Probe into gaseous pollution and assessment of air quality benefit under sector dependent emission control strategies over megacities in Yangtze River Delta, China. Atmos. Environ. 79, 841–852.

Dunker, A.M., Yarwood, G., Ortmann, J.P., Wilson, G.M., 2002. Comparison of source apportionment and source sensitivity of ozone in a three-dimensional air quality model. Environ. Sci. Technol. 36, 2953–2964.

Emery, C., Liu, Z., Russell, A.G., Odman, M.T., Yarwood, G., Kumar, N., 2017. Recommendations on statistics and benchmarks to assess photochemical model performance. J. Air Waste Manag. Assoc. 67, 582–598.

Emmons, L.K., Walters, S., Hess, P.G., Lamarque, J.-F., Pfister, G.G., Fillmore, D., Granier, C., Guenther, A., Kinnison, D., Lepple, T., Orlando, J., Tie, X., Tyndall, G., Wiedinmyer, C., Baughcum, S.L., Kloser, S., 2010. Description and evaluation of the model for ozone and related chemical tracers, version 4 (MOZART-4). Geosci. Model Dev. (GMD) 3, 43–67.

Feng, Z.Z., Sun, J.S., Wan, W.X., Hu, E.Z., Calatayud, V., 2014. Evidence of widespread ozone-induced visible injury on plants in Beijing, China. Environ. Pollut. 193, 296–301.

Feng, Z., Hu, E., Wang, X., Jiang, L., Liu, X., 2015. Ground-level O_3 pollution and its impacts on food crops in China: a review. Environ. Pollut. 199, 42–48.

Finlayson-Pitts, B.J., Pitts Jr., J.N., 1993. Atmospheric chemistry of tropospheric ozone formation: scientific and regulatory implications. Air Waste 43 (8), 1091–1100.

Gao, J., Zhu, B., Xiao, H., et al., 2016. A case study of surface ozone source apportionment during a high concentration episode, under frequent shifting wind conditions over the Yangtze River Delta, China. Sci. Total Environ. 544, 853–863.

Han, X., Zhu, L.Y., Wang, S.L., Meng, X.Y., Zhang, M.G., Hu, J., 2018. Modeling study of impacts on surface ozone of regional transport and emissions reductions over North China Plain in summer 2015. Atmos. Chem. Phys. 18, 12207–12221.

Huang, C., Chen, C.H., Li, L., Cheng, Z., Wang, H.L., Huang, H.Y., Streets, D.G., Wang, Y.J., Zhang, G.F., Chen, Y.R., 2011. Emission inventory of anthropogenic air pollutants and VOCs species in the Yangtze River Delta region, China. Atmos. Chem. Phys. 11, 4105–4120.

Li, L., Chen, C.H., Huang, C., Huang, H.Y., Zhang, G.F., Wang, Y.J., Wang, H.L., Lou, S.R., Qiao, L.P., Zhou, M., Chen, M.H., Chen, Y.R., Streets, D.G., Fu, J.S., Jang, C.J., 2012a. Process analysis of regional ozone formation over the Yangtze River Delta, China using the Community Multi-scale Air Quality modeling system. Atmos. Chem. Phys. 12 (22), 10971–10987.

Li, L., An, J.Y., Shi, Y.Y., Zhou, M., Yan, R.S., Huang, C., Wang, H.L., Lou, S.R., Wang, Q., Lu, Q., Wu, J., 2016. Source apportionment of surface ozone in the Yangtze River Delta, China in the summer of 2013. Atmos. Environ. 144, 194–207.

Li, Y., Lau, A.H., Fung, J.H., Zheng, J., Zhong, L., Louie, P.K.K., 2012b. Ozone source apportionment (OSAT) to differentiate local regional and super-regional source contributions in the Pearl River Delta region, China. J. Geophys. Res.: Atmosphere 117, D15305.

Li, Y., Lau, A.K.H., Fung, J.C.H., et al., 2013. Systematic evaluation of ozone control policies using an Ozone Source Apportionment method. Atmos. Environ. 76, 136–146.

Li, L., Chen, C., Huang, C., Huang, H.Y., Zhang, G.F., Wang, Y.J., Chen, M.H., Wang, H.L., Chen, Y.R., Streets, D.G., Fu, J.M., 2011. Ozone sensitivity analysis with the MM5-CMAQ modeling system for Shanghai. J. Environ. Sci. 23 (7), 1150–1157.

Li, M., Zhang, Q., Kurokawa, J.I., Woo, J.H., He, K.B., Lu, Z.F., et al., 2017. MIX: a mosaic Asian anthropogenic emission inventory under the international collaboration framework of the MICS-Asia and HTAP. Atmos. Chem. Phys. 17, 935–963.

Liang, X., Zou, T., Guo, B., Li, S., Zhang, H., Zhang, S., Huang, H., Chen, S.X., 2015. Assessing Beijing's $PM_{2.5}$ pollution: severity, weather impact, APEC and winter heating. Proc. R. Soc. A 471, 20150257. https://doi.org/10.1098/rspa.2015.0257.

Liu, T., Li, T.T., Zhang, Y.H., Xu, Y.J., Lao, X.Q., Rutherford, S., Chu, C., Luo, Y., 2013. The short-term effect of ambient ozone on mortality is modified by temperature in Guanzhou, China. Atmos. Environ. 76, 59–67.

Liu, Y., Li, L., An, J.Y., Zhang, W., Yan, R.S., Huang, L., Huang, C., Wang, H.L., Wang, Q., Wang, M., 2018. Emissions, chemical composition, and spatial and temporal allocation of the BVOCs in the Yangtze River Delta Region in 2014. Environ. Sci. 39 (2), 607–616.

Liu, X.-H., Zhang, Y., Xing, J., Zhang, Q., Wang, K., Streets, D.G., et al., 2010. Understanding of regional air pollution over China using CMAQ, part II. Process analysis and sensitivity of ozone and particulate matter to precursor emissions. Atmos. Environ. 44, 3719–3727.

Ou, J., Yuan, Z., Zheng, J., Huang, Z., Shao, M., Li, Z., et al., 2016. Ambient ozone control in a photochemically active region: short-term despising or long-term attainment? Environ. Sci. Technol. 50, 5720–5728.

Qin, Y., Wagner, F., Scovronicka, N., Peng, W., Yang, J.N., Zhu, T., Smith, K.R., Mauzerall, D.L., 2017. Quality, health, and climate implications of China's synthetic natural gas development. Proc. Natl. Acad. Sci. Unit. States Am. 114, 4887–4892.

Qu, Y., An, J., Li, J., Chen, Y., Li, Y., Liu, X., et al., 2014. Effects of NOx and VOCs from five emission sources on summer surface O3 over the Beijing-Tianjin-Hebei region. Adv. Atmos. Sci. 31, 787–800.

Shao, M., Tang, X.Y., Zhang, Y.H., Li, W.J., 2006. City clusters in China: air and surface water pollution. Front. Ecol. Environ. 4 (7), 353–361.

Shen, J., Zhang, Y., Wang, X., et al., 2015. An ozone episode over the Pearl River Delta in October 2008. Atmos. Environ. 122, 852–863.

Simon, H., Baker, K.R., Phillips, S., 2012. Compilation and interpretation of photochemical model performance statistics published between 2006 and 2012. Atmos. Environ. 61, 124–139.

Tang, X., Zhu, J., Wang, Z.F., et al., 2011. Improvement of ozone forecast over Beijing based on ensemble Kalman filter with simultaneous adjustment of initial conditions and emissions. Atmos. Chem. Phys. 11 (24), 12901–12916.

Turnock, S.T., Wild, O., Dentener, F.J., Davila, Y., Emmons, L.K., Flemming, J., Folberth, G.A., Henze, D.K., Jonson, J.E., Keating, T.J., Kengo, S., Lin, M., Lund, M., Tilmes, S., O'Connor, F.M., 2018. The impact of future emission policies on tropospheric ozone using a parameterised approach. Atmos. Chem. Phys. 18, 8953–8978.

Wang, X.S., Li, J.L., Zhang, Y.H., et al., 2009a. Ozone source attribution during a severe photochemical smog episode in Beijing, China. Sci. China, Ser. B: Chemistry 52 (8), 1270–1280.

Wang, X., Chen, F., Wu, Z., et al., 2009b. Impacts of weather conditions modified by urban expansion on surface ozone: comparison between the Pearl River Delta and Yangtze River Delta regions. Adv. Atmos. Sci. 26 (5), 962–972.

Wang, N., Guo, H., Jiang, F., et al., 2015. Simulation of ozone formation at different elevations in mountainous area of Hong Kong using WRF-CMAQ mode. Sci. Total Environ. 505, 939–951.

Wang, Y., Shen, L., Wu, S., Mickley, L., He, J., Hao, J., 2013. Sensitivity of surface ozone over China to 2000–2050 global changes of climate and emissions. Atmos. Environ. 75, 374–382.

Wang, T., Xue, L.K., Brimblecombe, P., Yun, F.L., Li, L., Zhang, L., 2017. Ozone pollution in China: a review of concentrations, meteorological influences, chemical precursors, and effects. Sci. Total Environ. 575, 1582–1596.

Wu, Q., Wang, Z., Chen, H., et al., 2012. An evaluation of air quality modeling over the Pearl River Delta during November 2006. Meteorol. Atmos. Phys. 116 (3–4), 113–132.

Xing, J., Wang, S.X., Jang, C., Zhu, Y., Hao, J.M., 2011. Nonlinear response of ozone to precursor emission changes in China: a modeling study using response surface methodology. Atmos. Chem. Phys. 11, 5027–5044.

Yarwood, G., Morris, R.E., Yocke, M.A., Hogo, H., Chico, T., 1996. Development of a methodology for source apportionment of ozone concentration estimates from a photochemical grid model. In: Presented at the 89th AWMA Annual Meeting, Nashville TN, June 23-28.

Yarwood, G., Koo, B., 2015. Improved OSAT, APCA and PSAT Algorithms for CAMx. Final Report Prepared for the Texas Commission on Environmental Quality, Austin, Texas (August, 2015). Prepared by Ramboll Environ, Novato, CA.

Zhang, H., Wang, Y., Hu, J., Ying, Q., Hu, X.M., 2015. Relationships between meteorological parameters and criteria air pollutants in three megacities in China. Environ. Res. 140, 242–254.

Zhang, L., Wang, T., Zhang, Q., Zheng, J., Xu, Z., Lv, M., 2016. Potential sources of nitrous acid (HONO) and their impacts on ozone: a WRF-Chem study in a polluted subtropical region. J. Geophys. Res. Atmos. 121 2015JD024468.